Contribution of Evanescent Waves to Vortex Vector Field with Inhomogeneous Polarization in Near Field

Yin-Long Feng[1] **and Rui-Pin Chen**[1, 2]

[1]School of Sciences, Zhejiang A & F University, Lin'an, Zhejiang 311300, China
[2]Department of Physics, Zhejiang Sci-Tech University, Hangzhou 310018, China

Abstract— We study the evanescent wave of a vortex vector optical field with inhomogeneous states of polarization in the cross section of the field. The TE and TM terms of the evanescent wave and the propagating wave of a cylindrical vortex vector optical field with inhomogeneous states of polarization in the cross section of the field are derived by the vector angular spectrum method. The vector structure of the evanescent wave and propagating wave components of the cylindrical vector field is demonstrated. The ratio of the evanescent wave and the propagating wave of a cylindrical vector optical field with different states of polarization with different vortex charges n and polarization charges m as a function of propagation distance in near field is described. Comparison between the contribution of TE and TM terms of both the propagating and the evanescent waves of the cylindrical vortex vector field in free space is demonstrated. The intensity (squared modulus) distributions of the TE and TM terms of the propagating and evanescent waves are described to compare the contributions of the propagating and the evanescent waves associated with the cylindrical vector field with inhomogeneous states of polarization in the cross section of the field. These results, therefore, provide useful information on how to spatially manipulate the evanescent waves of a vortex vector cylindrical optical field in near field by choosing appropriate vortex charges n and states of polarization in the cross-section of the field.

Recently, the vector optical field with the different states of polarization in the cross-section of the field has attracted much interest in linear and nonlinear optics realms due to its novel properties and potential application [1, 2]. In the Cartesian coordinate system, the z-axis is taken to be the propagation axis. A cylindrical optical vector field is expressed as [1, 2]

$$E(r,\theta) = A(r,\theta)[\cos(m\theta+\theta_0)e_x + \exp(i\Delta\theta)\sin(m\theta+\theta_0)e_y], \tag{1}$$

where $r = \sqrt{x^2+y^2}$ and $\theta = \arctan(y/x)$ are the polar radius and azimuthal angle in the polar coordinate system, respectively. m is the topological charge, and θ_0 is the initial phase. e_x and e_y are the unit vectors in x and y-direction, respectively. m is the topological charge, and θ_0 is the initial phase. e_x, e_y and e_z are the unit vectors in x, y and z-direction, respectively. When $m = 1$ with $\theta_0 = 0$ and $\pi/2$, the vector fields describe the radially and azimuthally polarized vector fields, respectively. When $m = 0$, Eq. (1) degenerate to the linearly-polarized fields. $A(r)$ represents the amplitude distribution in the cross-section of the cylindrical vector field. For the case with $\Delta\theta \neq 0$ (Eq. (1)), however, the x- and y-components have different phase, indicating a hybrid-polarized vector field with the linear, circular and elliptical polarization states located at different position in the field cross-section.

For the Gaussian distribution with the n-th vortex and an arbitrary polarized electromagnetic field (see Eq. (1)) in the source plane $z = 0$, $A(r,\theta) = \exp(-r^2/w^2)\exp(in\theta)$ where w is beam-width. By using the Fourier transform, the angular spectrum is

$$\begin{aligned} A(\rho\cos\phi,\rho\sin\phi) \;=\; & Q\,\{P\exp[i(m\phi+n\phi+\theta_0)](e_x - i\exp(i\Delta\theta)e_y) \\ & +T\exp\left[-i\left(m\phi-n\phi+\theta_0\right)\right]\left(e_x+i\exp(i\Delta\theta)e_y\right) \\ & -\left[P\exp[i(m\phi+n\phi+\theta_0)]\left(\cos\phi - i\exp(i\Delta\theta)\sin\phi\right)\right. \\ & \left.+T\exp\left[-i\left(m\phi-n\phi+\theta_0\right)\right]\left(\cos\phi+i\exp(i\Delta\theta)\sin\phi\right)\right]\rho/\gamma e_z\} \end{aligned} \tag{2}$$

with

$$\begin{aligned} \mathrm{P} &= I_{(m+n-1)/2}\left(k^2w^2\rho^2/8\right) - I_{(m+n+1)/2}\left(k^2w^2\rho^2/8\right) \\ \mathrm{T} &= I_{(m-n-1)/2}\left(k^2w^2\rho^2/8\right) - I_{(m-n+1)/2}\left(k^2w^2\rho^2/8\right) \\ Q &= \pi i^{m+n}\left(\frac{k}{2\pi}\right)^2 \frac{\sqrt{\pi}kw^3\rho}{8}\exp(-k^2w^2\rho^2/8) \end{aligned}$$

where k is the wavenumber $I(\cdot)$ are the Bessel functions of the second kind and e_z is the unit vector in z direction. The electric field component of the vector cylindrical optical field in z plane can be represented as

$$\begin{aligned}
&E(r) = (-1)^{m+n}\frac{k^3w^3\sqrt{\pi}}{16}\int_0^\infty e^{-\frac{k^2w^2\rho^2}{8}}\,\{P\ J_{m+n}(-kr\rho)\exp[i(m\theta+n\theta+\theta_0)](e_x - i\exp(i\Delta\theta)e_y)\\
&+TJ_{m-n}(-kr\rho)\exp[-i(m\theta-n\theta+\theta_0)](e_x+i\exp(i\Delta\theta)e_y)\\
&+[PJ_{m+n+1}(-kr\rho)\exp[i(m\theta+n\theta+\theta+\theta_0)](1-\exp(i\Delta\theta))\\
&+PJ_{m+n-1}(-kr\rho)\exp[i(m\theta+n\theta-\theta+\theta_0)](1+\exp(i\Delta\theta)))\\
&+TJ_{m-n-1}(-kr\rho)\exp[-i(m\theta-n\theta-\theta+\theta_0)](1+\exp(i\Delta\theta))\\
&+TJ_{m-n+1}(-kr\rho)\exp[-i(m\theta-n\theta+\theta+\theta_0)](1-\exp(i\Delta\theta))\ ]i\rho/2\gamma e_z\}\times\exp\left(ik\gamma z\right)\rho^2 d\rho \qquad (3)
\end{aligned}$$

In order to compare the contributions of the propagating and the evanescent waves associated with the cylindrical vector field, the integrated intensity (squared modulus) of the propagating and evanescent fields, I_{pr} and I_{ev}, are calculated respectively [3, 4]:

$$I_{pr} = \iint |E_{pr}|^2 dxdy = \int_0^1\int_0^{2\pi}\left[|a|^2+|b|^2\right]\rho d\rho d\phi, \qquad (4)$$

$$I_{ev} = \iint |E_{ev}|^2 dxdy = \int_1^\infty\int_0^{2\pi}\left[|a|^2+|b_{ev}|^2\right]\exp(-2kz\sqrt{\rho^2-1})\rho d\rho d\phi, \qquad (5)$$

with

$$a = A(\rho,\phi)\cdot e_1 \quad b = A(\rho,\phi)\cdot e_2 \quad b_{ev} = A(\rho,\phi)\cdot e_{ev},$$

For $m = 1$,

$$I_{pr} = 2\pi\int_0^1 |Q|^2\left[\left(P^2+T^2\right)\left(2-\rho^2\right)+2\rho^2 PT\cos^2\left(\Delta\theta/2\right)\cos\left(2\theta_0\right)\right]/\left(1-\rho^2\right)\rho d\rho \qquad (6)$$

$$\begin{aligned}
I_{ev} &= 2\pi\int_1^\infty |Q|^2\left[\left(P^2+T^2\right)\left(2-3\rho^2+2\rho^4\right)+2\left(3\rho^2-2\rho^4\right)PT\cos^2\left(\Delta\theta/2\right)\cos\left(2\theta_0\right)\right]\\
&\quad\frac{\exp\left(-2kz\sqrt{\rho^2-1}\right)\rho}{1-3\rho^2+2\rho^4}d\rho \qquad (7)
\end{aligned}$$

For $m > 1$,

$$I_{pr} = 2\pi\int_0^1 |Q|^2\left[\left(P^2+T^2\right)\left(2-\rho^2\right)\right]/\left(1-\rho^2\right)\rho d\rho \qquad (8)$$

$$I_{ev} = 2\pi\int_1^\infty |Q|^2\left(P^2+T^2\right)\frac{\left(2-3\rho^2+2\rho^4\right)\exp\left(-2kz\sqrt{\rho^2-1}\right)}{1-3\rho^2+2\rho^4}\rho d\rho \qquad (9)$$

The substitution of Eqs. (4)–(7) into Eqs. (8) and (9), and performing integration over Ø from zero to 2π yield a single integration of ρ. Then, the corresponding results can be obtained by performing numerical integration over ρ. The ratio $\delta = (I_{pr} - I_{ev})/I_{pr}$ provides direct information about the propagating and evanescent components of the field.

The ratio $\delta = (I_{pr} - I_{ev})/I_{pr}$ for $w = 0.1\lambda$ (highly non-paraxial case) and $w = 0.5\lambda$ cases as a function of different distances z from the initial plane $z = 0$ are shown in the Fig. 1. The evanescent field dominates near the source plane and the relative weight of $\mathbf{I}_{ev}$ would drastically decrease with the increasing propagation distance. Thus it can be negligible in the propagation distance $z = 0.5\lambda$ as shown in Fig. 1. Comparing Figs. 1(a) with (b), one can recognize that the relative weight of I_{ev} would reduce when the waist size w increases. i.e., the relative weight of the evanescent wave component is increasing with increasing non-paraxial as the waist size w decreases. The relative weight of I_{ev} would increase with the increasing topological charge. It can be explained that the field distribution will increasingly diverge and extend from the center of beam with the increasing topological charge. As a result, the relative weight of I_{ev} would increase with the increasing topological charge under the same conditions and beam parameters.

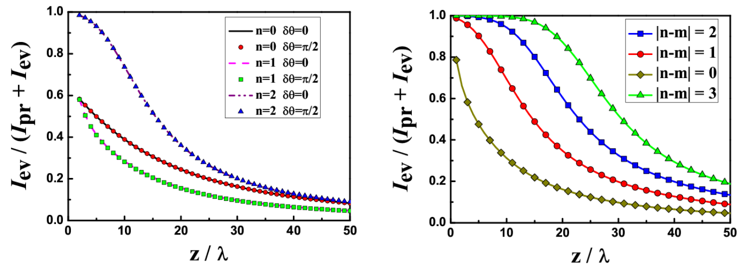

(a) (b)

Figure 1: Ratio of the propagating and evanescent components of the field as a function of the propagation distances with (a) $m = 1$; (b) $m = 2$, 3.

The calculation results indicate that the evanescent wave component with different initial phase θ_0 for any topological charge (except $m = 1$) is same as shown in Fig. 1. For $m = 1$ case with different initial phase θ_0, the relative weight of I_{ev} of the azimuthal polarization ($m = 1$, $\theta = \pi/2$) is maximum and the relative weight of I_{ev} of the radial polarization ($m = 1$, $\theta = 0$) is minimum as shown in Fig. 1. The physical explanation for the exception $m = 1$ is that the values of z-components of either propagation wave or evanescent wave are different with the different initial phase θ_0, the values of z-components of either propagation wave or evanescent wave are maximum for $\theta_0 = \pi/2$ (i.e., radial polarization) whereas the z-components of either propagation wave or evanescent wave are zero for $\theta_0 = 0$ (i.e., azimuthal polarization).

REFERENCES

1. Zhan, Q. W., "Cylindrical vector beams: From mathematical concepts to applications," *Adv. Opt. Photon.*, Vol. 1, 1–57, 2009.
2. Wang, X. L., Y. N. Li, J. Chen, C. S. Guo, J. P. Ding, and H. T. Wang, "A new type of vector fields with hybrid states of polarization," *Opt. Express*, Vol. 18, 10786–10795, 2010.
3. Martínez-Herrero, R., P. M. Mejías, S. Bosch, and A. Carnicer, "Vectorial structure of non-paraxial electromagnetic beams," *J. Opt. Soc. Am. A*, Vol. 18, 1678–1680, 2001.
4. Chen, R. P. and G. Li, "The evanescent wavefield part of a cylindrical vector beam," *Opt. Express*, Vol. 21, 22246–22254, 2013.